PERGAMON

International Journal of Solids and Structures 37 (2000) 5733–5744

INTERNATIONAL JOURNAL OF SOLIDS and STRUCTURES

www.elsevier.com/locate/ijsolstr

Finite solid circular cylinders subjected to arbitrary surface load. Part II — Application to double-punch test

X.X. Wei [a], K.T. Chau [b,*]

[a] *Department of Mechanics, Lanzhou University, Lanzhou 730000, People's Republic of China*
[b] *Department of Civil and Structural Engineering, The Hong Kong Polytechnic University, Hung Hom, Kowloon, Hong Kong, SAR, People's Republic of China*

Received 7 May 1999

Abstract

This paper derives the stress distributions within a finite isotropic solid circular cylinder of diameter $2b$ and length $2h$ under the double-punch test, which was introduced by Chen (1970) for the determination of the indirect tensile strength of concrete. The stresses induced by the two rigid circular punches of diameter $2a$ at the top and bottom of the solid cylinder are modeled by considering contact problem. The general stress analysis discussed in a companion paper (Part I) is used to obtain the stress field within the solid. In general, tensile stress concentrations are developed beneath the punches compared to the roughly uniform tensile stress at the central portion of the axis of the cylinder. The maximum tensile stress in the tensile zone decreases with the increase of Poisson's ratio and a/b, but is roughly independent of h/b. For small Poisson's ratio (say about 0.1) and a/b (say smaller than 0.1), the assertion made by Chen (1970) and Marti (1989) that a uniform tensile stress field, similar to that of the Brazilian test, is developed along the axis of symmetry is incorrect. The tensile strength interpreted from the present analysis is found comparable to the formula proposed by Bortolotti (1988) for $a/b > 0.2$ and agrees well with the experimental data, and thus provides an improvement over Chen's (1970) original formula.

Keywords: Double-punch test; Finite solid cylinders; Concrete; Elastic stress analysis

1. Introduction

In a companion paper (Chau and Wei, 1999c; below referred as CW), we have given a general approach for stress analysis within a finite isotropic elastic solid cylinder under arbitrary traction on its

* Corresponding author. Tel.: +852-2766-6015; fax: +852-2334-6389.
E-mail address: cektchau@polyu.edu.hk (K.T. Chau).

0020-7683/00/$ - see front matter
PII: S0020-7683(99)00290-5

end and curved surfaces. The applied traction, in general, can be non-axisymmetric. The equations of equilibrium are uncoupled by introducing two displacement functions. Appropriate series expressions, in terms of Bessel and modified Bessel functions, hyperbolic functions, and trigonometric functions, are proposed for the two displacement functions. Systems of simultaneous equations for determining the unknown constants in the series expressions of the two displacement functions are derived. A particular form of this solution technique has been applied to obtain the solutions for the diametral and axial Point Load Strength Tests (PLST) on cylinders by Chau (1998) and Chau and Wei (1999b), and by Wei et al. (1999), respectively. In the present study, we will apply the general solution derived in CW to consider the stress field in solid cylinders under the double-punch test.

The double-punch test was originally proposed by Chen (1970, 1975) for determining the indirect tensile strength of concrete. In this test, a concrete cylinder is placed vertically between the loading platens of a uniaxial compression machine and compressed by two steel circular punches located concentrically on the top and bottom surfaces of the cylinder (see Fig. 1). The solid cylinder normally fails by tensile splitting along several vertical diametral planes as shown in Fig. 8 of Chen and Yuan (1980). The double-punch test is believed to be more attractive than the conventional Brazilian test or the splitting test because: (1) the testing procedure is easier than that for the splitting test; (2) a smaller applied load is needed to fracture the specimen (i.e. a machine of smaller capacity can be used); and (3) the calculated tensile strength in a double-punch test gives an average of strength on several cracked diametral planes, compared to one fracture plane in the splitting test. Experimental results show that size effect on the tensile strength is important in the double-punch test. In particular, for a fixed geometric ratio, it is observed that a larger specimen size will result in a smaller tensile strength (Hyland

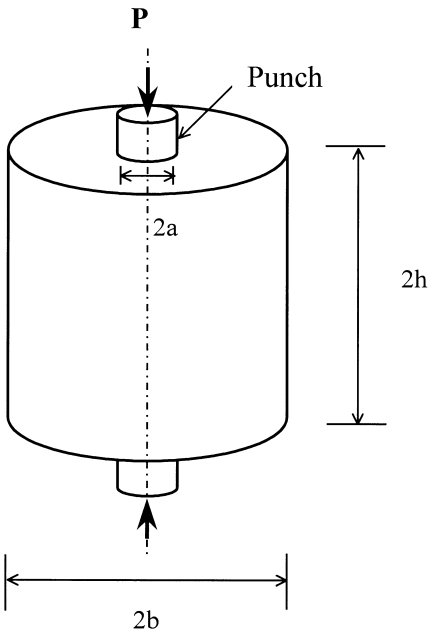

Fig. 1. A sketch of a finite solid circular cylinder of length $2h$ and diameter $2b$ compressed between a pair of rigid circular punches on the top and bottom surfaces. The diameter of the punches is $2a$, and the applied force is denoted by P.

and Chen, 1970; Chen and Yuan, 1980; Marti, 1989). However, the tensile strength interpreted from the double-punch test is relatively insensitive to the shape of the specimens (Chen and Trumbauer, 1972; Chen and Yuan, 1980). It is also concluded that the size of the punches is not important as long as a/b is roughly 1/4, where a and b are the radii of the punches and the solid cylinder, respectively (Chen and Trumbauer, 1972; Chen and Yuan, 1980). The double-punch test has been done on cylinders of mortar, plain concrete, fiber reinforced concrete and polymer impregnated concrete (Chen and Yuan, 1980; Chen and Colgrove, 1974).

To interpret the indirect tensile strength from the double-punch test, Chen (1970) applied the limit analysis of perfectly plastic material by Chen and Drucker (1969) and obtained the following approximation:

$$f_t = \frac{P}{\pi(1.2bH - a^2)} \tag{1}$$

where $H = 2h$ is the height of the cylinder, and P is the applied load at failure.

Based on Bazant's (1984) non-linear fracture mechanics approach, Marti (1989) proposed the following tensile strength for the double-punch test:

$$f_t = 0.4\frac{P}{4b^2}\sqrt{1 + \frac{2b}{\lambda d_a}} \tag{2}$$

where d_a is the maximum aggregate size and λ is an empirical constant depend on the type of material (ranging from 37 to 68 for concrete). It should be noted that for small specimen size the square-root term in Eq. (2) can be approximated by 1 when the size effect can be neglected.

By assuming a modified Coulomb-like failure criterion for concrete, Bortolotti (1988) proposed the following formula for the tensile strength for the double-punch test:

$$f_t = \frac{P}{\pi(bH - a^2\cot\alpha)} \tag{3}$$

where α is defined as

$$\alpha = \frac{\pi}{2} - \frac{\phi}{2} \tag{4}$$

Here, ϕ is the shearing resistance angle in the modified Coulomb's yield criterion; its typical value is 53° leading to $\alpha = 18.5^\circ$ (Bortolotti, 1988).

By applying the finite element analysis of Chen and Chen (1976), Chen and Yuan (1980) proposed the following approximation by assuming the cylinder as a linear elastic, plastic strain-hardening and fracture material:

$$f_t = \frac{0.75P}{\pi(1.2bH - a^2)} \tag{5}$$

which is interpreted from the maximum tensile stress along the axis of symmetry for the case of $a/b = 1/4$ and $b/h = 1$.

There is, however, no exact solution for the elastic tensile stress within a solid circular cylinder under the double-punch test. Thus, the main objective of this paper is to obtain such solution using the exact analysis proposed in CW. The solution will be used to interpret the tensile strength of concrete from the

double-punch test and to compare the approximate formulas proposed by Chen (1970) and Bortolotti (1988) given in Eqs. (1) and (3).

2. Boundary conditions and contact stress

The only non-zero tractions on the surfaces of the cylinder shown in Fig. 1 are the stresses induced by the two rigid circular punches acting at the top and bottom end surfaces. If the traction caused by each punch acting on the cylinder is modeled by contact stress between a smooth rigid circular punch and a flat half-space (by assuming no frictional contact), the following formula can be used (Sneddon, 1951):

$$\sigma_{zz} = \begin{cases} -p(r) & r < a \\ 0 & r > a \end{cases} \tag{6}$$

where

$$p(r) = \frac{P}{2a\pi\sqrt{a^2 - r^2}} \tag{7}$$

where P is the magnitude of the applied point force. The contact stress becomes singular or unbounded at the edge of the contact zone ($r = a$), and it is also independent of the elastic properties of the cylinders.

Therefore, the boundary conditions for a solid cylinder subjected to the double-punch test are:

$$\sigma_{rr} = 0, \quad \sigma_{rz} = 0 \qquad \text{on } r = R \tag{8}$$

$$\sigma_{rz} = 0, \quad \sigma_{zz} = \begin{cases} -p(r) & r < a \\ 0 & r > a \end{cases} \qquad \text{on } z = \pm h \tag{9}$$

where $p(r)$ is the contact pressure given in Eq. (7).

In order to apply the results obtained in CW, the normal boundary traction on $z = \pm h$ is first expanded into Fourier–Bessel series (Watson, 1944):

$$\sigma_{zz} = -\frac{P}{\pi ab}\sum_{s=1}^{\infty}\frac{\sin(\lambda_s a/b)}{\lambda_s J_0^2(\lambda_s)}J_0(\lambda_s \rho) \tag{10}$$

where $\rho = r/b$ and λ_s is the sth root of $J_1(x) = 0$, and $J_n(x)$ is the Bessel function of order n (Abramowitz and Stegun, 1965). The derivation for this expansion is outlined in Appendix A.

3. Series expressions for the two displacement functions

For axisymmetric problems (i.e. all variables and displacement functions are independent of θ), it is straightforward to see that the shear stresses $\sigma_{z\theta}$ and $\sigma_{r\theta}$, and the displacement function Ψ are identically zero. And, we can set $\omega_n = 0$ and $k = l = 1$ in Eq. (24) of CW; in addition, to simplify our notation the superscript (1) is dropped in the following expressions. Note in addition that the summation for n disappears since the present problem is axisymmetric (i.e. $\omega_n = 0$). More specifically, the following series representation for the displacement function Φ can be specialized from Eq. (24) of CW:

$$\Phi = -\frac{b^3}{2G}\left\{A_0\frac{\kappa^3\zeta^3}{6} + C_0\frac{\kappa\zeta\rho^2}{2} + \sum_{m=1}^{\infty}\frac{\sin(m\pi\zeta)}{\eta_m^3}\left[A_m\eta_m\rho I_1(\eta_m\rho) + B_m I_0(\eta_m\rho)\right]\right.$$
$$\left. + \sum_{s=1}^{\infty}\frac{J_0(\lambda_s\rho)}{\lambda_s^3}\left[C_s\sinh(\gamma_s\zeta) + D_s\gamma_s\zeta\cosh(\gamma_s\zeta)\right]\right\} \tag{11}$$

where the two normalized coordinates ρ and ζ are defined as $\rho = r/b$ and $\zeta = z/h$; κ is a geometrical shape ratio defined as $\kappa = h/b$; λ_s is the sth root of $J_1(x) = 0$; $\gamma_s = \lambda_s\kappa$ and $\eta_m = m\pi/\kappa$; $J_0(x)$, $J_1(x)$, $I_0(x)$ and $I_1(x)$ are Bessel and modified Bessel functions of the first kind of zero- and first-order, respectively; A_0, C_0, A_m, B_m, C_s and D_s are unknown coefficients to be determined.

4. Determination of unknown coefficients

Since the determination of the unknown coefficients has been discussed in detail by CW, we only compile the corresponding governing equations for these constants.

In particular, the following equations for BC11 (listed in Table 1 of CW) are specialized from Eqs. (47) and (50) of CW, respectively:

$$(2\nu - 1)C_0 + \nu A_0 = 0 \tag{12}$$

$$A_m\left[2\nu I_0(\eta_m R) - \frac{2}{\eta_m^2}\frac{\partial^2 I_0(\eta_m R)}{\partial r^2} - \frac{R}{\eta_m^2}\frac{\partial^3 I_0(\eta_m R)}{\partial r^3}\right] - \frac{B_m}{\eta_m^2}\frac{\partial^2 I_0(\eta_m R)}{\partial r^2}$$
$$+ \sum_{s=1}^{\infty}\left\{-\left[\left(C_s + (2\nu+1)D_s\right)\Gamma_s^{(1)} + D_s A_s^{(1)}\right]J_0(\gamma_s R)\right\} = 0 \tag{13}$$

Table 1
Comparison of the normalized tensile strength f_t/σ_0 interpreted from formulas by Chen (1970), Bortolotti (1988), and the present analysis (using $\nu = 0.15$ and 0.20) for various values of b/h and a/b

b/h	a/b	f_t/σ_0			
		Chen (1970)	Bortolotti (1988)	Present	
				$\nu = 0.15$	$\nu = 0.20$
1.0	0.30	0.551	0.736	0.657	0.638
1.0	0.25	0.545	0.703	0.723	0.688
1.0	0.20	0.545	0.677	0.858	0.781
1.0	0.10	0.545	0.647	2.260	1.794
1.5	0.30	0.363	0.430	0.470	0.440
1.5	0.25	0.545	0.453	0.567	0.517
1.5	0.20	0.545	0.442	0.733	0.645
1.5	0.10	0.545	0.429	2.162	1.700
0.7	0.30	0.801	1.126	0.887	0.838
0.7	0.25	0.788	1.050	1.010	0.956
0.7	0.20	0.788	0.995	1.154	1.072
0.7	0.10	0.788	0.930	2.630	2.158

The following equation for BC12 (see Table 1 of CW) is specialized from Eq. (52) of CW:

$$A_m\left[(3-2\nu)\frac{\partial I_0(\eta_m R)}{\partial r}+R\frac{\partial^2 I_0(\eta_m R)}{\partial r^2})\right]+B_m\frac{\partial I_0(\eta_m R)}{\partial r}=0 \tag{14}$$

The following equations for BC22 (see Table 1 of CW) are specialized from Eqs. (79) and (80) of CW:

$$2(2-\nu)C_0+(1-\nu)A_0=0 \tag{15}$$

$$\sum_{m=1}^{\infty}\left\{A_m\left[2(2-\nu)T_{sm}+U_{sm}\right]+B_m T_{sm}\right\}(-1)^m-\left\{\left[C_s+(2\nu-1)D_s\right]\cosh(\gamma_s L)+D_s\gamma_s L\sinh(\gamma_s L)\right\}=-\frac{P\sin(\lambda_s a/b)}{\pi ab\lambda_s J_0^2(\lambda_s)} \tag{16}$$

Finally, the following equation for BC21 (see Table 1 of CW) is specialized from Eq. (84) of CW:

$$(C_s+2\nu D_s)\sinh(\gamma_s L)+D_s\gamma_s L\cosh(\gamma_s L)=0 \tag{17}$$

Thus, the four constants A_m, B_m, C_s and D_s can be evaluated by solving Eqs. (13), (14), (16) and (17), while C_0 and A_0 can be obtained by solving Eqs. (12) and (15) and they are obviously zeros for the present problem.

5. Numerical results and discussion

As noted by Chen and Yuan (1980), all vertical fracture planes pass through the axis of symmetry, therefore, the tensile stress appears to be the most important along this axis. Thus, only the stress distributions along the vertical axis will be calculated in this section. In addition, since the radial stress is the same as the hoop stress along the axis of cylinder for axisymmetric problems, only hoop stress will be considered here. The strategy for the evaluation of λ_s, or the sth root of $J_1(x)=0$, has been discussed in Section 8 of CW and will not be repeated here.

The infinite series in our solution has to be truncated to finite terms when numerical results are considered. To check the convergence of our series solution, Figs. 2 and 3 show the normalized hoop and axial stresses along the axis of symmetry versus the normalized distance z/h for various values of N (the number of terms used for the summation in both m and s). Since the stresses are symmetric with respect to z, only one half of the axis is plotted. In Fig. 2, the stresses are normalized with respect to $\sigma_0=P/(4b^2)$ and the plot is for $\nu=0.1$, $a/b=0.05$ and $b/h=1$. Similar to the numerical calculations for spheres under the PLST considered by Wijk (1978), Wei and Chau (1998) and Chau and Wei (1999a), the maximum tensile stress induced beneath the punch cannot be estimated accurately if the number of terms N is less than 20. For $N>20$, the solution, however, converges rapidly, as the approximations from adding 20 and 25 terms cannot be distinguished easily from Fig. 2. For $a/b=1/4$ and $b/h=1$ (the punch and specimen sizes suggested by Chen and Yuan, 1980), Fig. 3 shows that the tensile stress is roughly constant in the central portion of the axis of symmetry and the corresponding solution converges much faster. The approximation for $N=5$ basically coincides with those for $N=20$ and 25. Therefore, 25 terms in the summation should be sufficient to ensure the convergence of our numerical results. Note that as long as finite terms are used in the series solution, the contact stress will remain bounded even at the edge of the contact (compare Eq. (7)).

Fig. 4 plots the normalized tensile hoop stress and compressive axial stress versus the normalized

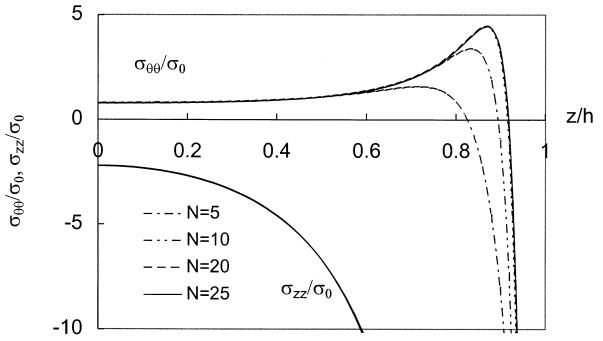

Fig. 2. The normalized hoop and axial stresses versus the normalized vertical coordinate z/h for approximations using various values of N, which is the number of terms used in the series summation. The stresses are normalized with respect to $\sigma_0 = P/(4b^2)$. Other parameters used are $b/h = 1$, $\nu = 0.1$ and $a/b = 0.05$.

distance measured from the center of the cylinder for various values of Poisson's ratio ν. The plot is for $a/b = 0.1$ and $b/h = 1$. For $\nu = 0.4$, tensile stress is roughly uniform as expected by Chen and Yuan (1980) and Marti (1989); but for $\nu \leq 0.3$, a zone of tensile stress concentration rises from the roughly uniform tensile stress at the central portion of the axis of symmetry. This finding contrasts the common belief that a uniform tensile stress field is developed along the vertical planes containing the cylinder axis (e.g. Marti, 1989; Chen and Yuan, 1980), but is similar to those for the axial PLST obtained by Wei et al. (1999).

Fig. 5 plots the normalized hoop and axial stresses versus the normalized distance z/h for various sizes of the punches (in terms of a/b). The following parameters are assumed: $\nu = 0.1$ and $b/h = 1$. It is clear that when $a/b = 0.25$ (as recommended by Chen and Yuan, 1980), the stress is uniform and the maximum tensile stress is developed at the center. However, for smaller punch size ($a/b < 0.125$), a zone of tensile stress concentration is developed beneath the two punches.

The shape effect on the maximum tensile stress is illustrated in Fig. 6, which plots the normalized stresses versus z/h for various values of h/b. The parameters used are: $\nu = 0.1$ and $a/b = 0.1$. Fig. 6 shows that the location of the peak tensile stress shifts towards the punch at the end surfaces when the height of the cylinder is increased, while the maximum is relatively insensitive to h/b. That is, the tensile

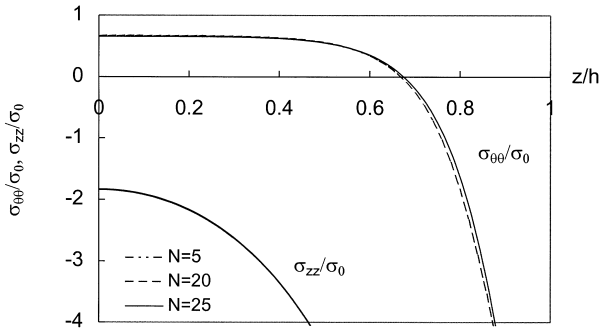

Fig. 3. The normalized hoop and axial stresses versus the normalized vertical coordinate z/h for approximations using various values of N, which is the number of terms used in the series summation. Other parameters used are $b/h = 1$, $\nu = 0.1$ and $a/b = 0.25$.

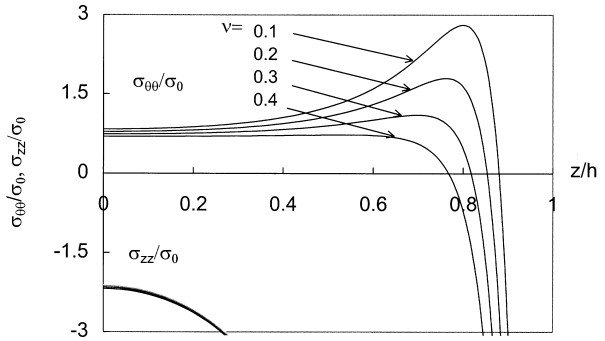

Fig. 4. The normalized hoop and axial stresses versus the normalized vertical coordinate z/h for various values of Poisson's ratio. Other parameters used are $b/h = 1$ and $a/b = 0.1$.

strength obtain in the double-punch test is insensitive to the exact shape of the cylinder. This conclusion agrees with the experimental observation, by Chen and Yuan (1980), that shape effect on the tensile strength of the cylinder is not very significant. Of course, if a very slender cylinder is loaded and if the top and bottom punches are not exactly concentric, large deformation may occur and buckling stresses may be induced. Thus, the apparent tensile strength will be much smaller.

To further investigate the size effect, we fix the shape ($h/b = 1$), the size of the punches ($a = 2.5$ mm), and the Poisson's ratio ($\nu = 0.1$) in Fig. 7, which plots the normalized stresses versus z/h for various values of $2b$. The maximum tensile stress increases with the diameter of the cylinder, thus a smaller tensile strength will be resulted. This size effect has been observed in experiments, as noted by Chen and Yuan (1980) and Marti (1989).

One of the main differences between the present prediction and those given in Eqs. (1)–(4) is that the tensile strength interpreted from our solution depends on Poisson's ratio of the tested material. Fig. 8 plots the normalized stresses versus z/h for various values of Poisson's ratio. The parameters used are $h/b = 1$ and $a/b = 0.25$, which are the parameters recommended by Chen and Yuan (1980). Fig. 8 shows that the maximum tensile stress decreases with Poisson's ratio. Noted that although the tensile stress along the axis is roughly constant, the maximum is not necessarily at the center of the cylinder.

To compare the prediction by the present analysis and those predicted by others, Table 1 tabulates

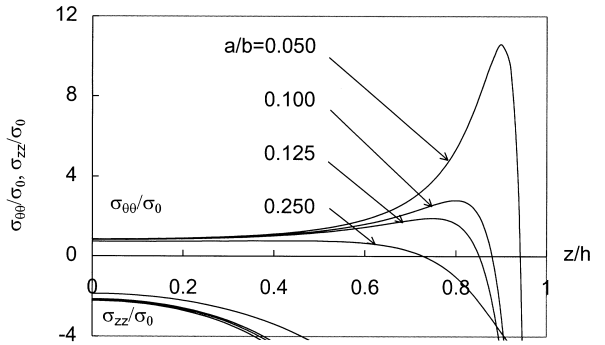

Fig. 5. The normalized hoop and axial stresses versus the normalized vertical coordinate z/h for various values of size of punches in terms of a/b. Other parameters used are $b/h = 1$ and $\nu = 0.1$.

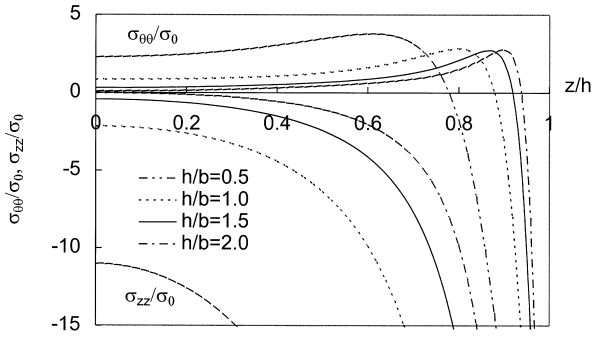

Fig. 6. The normalized hoop and axial stresses versus the normalized vertical coordinate z/h for various values of shape factor h/b. Other parameters used are $a/b = 0.1$ and $\nu = 0.1$.

the normalized tensile strengths calculated by using formulas proposed by Chen (1970) and Bortolotti (1988), together with our predictions for $\nu = 0.15$ and 0.2 for various values of h/b and a/b. This range of Poisson's ratio should cover the typical value for most concrete (e.g. Neville, 1978). From Table 1, we conclude that for $b/h = 1$ and $a/b > 0.2$, $b/h = 1.5$ and $a/b = 0.3$, and $b/h = 0.7$ and $a/b = 0.25$ our predictions are comparable to those given by Bortolotti (1988). Therefore, the estimation by Bortolotti's (1988) formula appears to be more comparable to our prediction for $a/b > 0.25$, but appears to underestimate the tensile strength for smaller a/b. The estimation by Chen (1970) is found comparable to ours only when $b/h = 0.7$ and $a/b = 0.3$. Generally speaking, our predictions agree better with those given by Bortolotti (1988) than with those by Chen (1970), which seems to underestimate the tensile strength for all values of b/h and a/b. To investigate the range of applicability of our solution, especially for changing b/h and a/b, more thorough experimental studies are required.

Since Bortolotti (1988) concluded that predictions of his formula agree better with experiments than those by Chen (1970), we expect that our prediction should also agree well with the experimental observation. One way to check the validity of our solution is to calibrate the tensile strength of concrete from a single data of a batch of experiments, and to predict the loads at failure for the rest of the batch. Table 2 presents a comparison of our predicted fracture loads and the experimental observations by Hyland and Chen (1970) for concrete specimens of various shapes under punches of various sizes. The observed fracture load ($P = 161.1$ kN) for the concrete solid cylinder with $a/b = 0.2484$ and $h/b = 1$ is

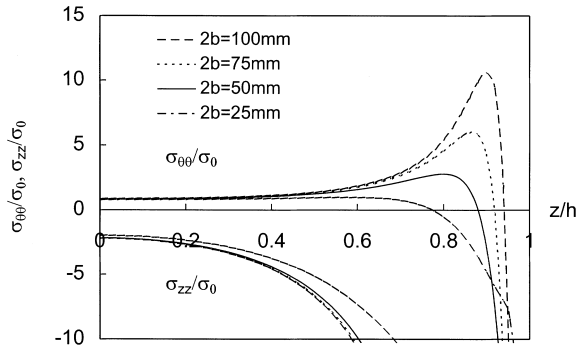

Fig. 7. The normalized hoop and axial stresses versus the normalized vertical coordinate z/h for various diameters of the cylinder $2b$. Other parameters used are $h/b = 1$, $a/b = 0.1$ and $\nu = 0.1$.

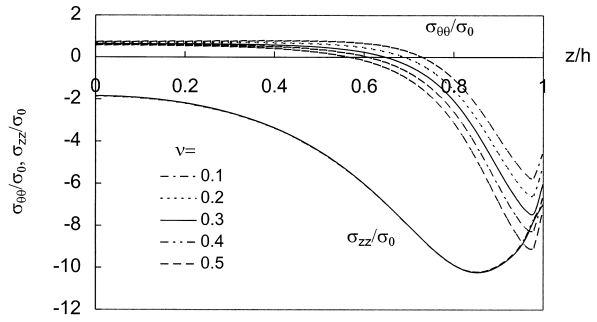

Fig. 8. The normalized hoop and axial stresses versus the normalized vertical coordinate z/h for various values of Poisson's ratio. Other parameters used are $a/b = 0.25$ and $h/b = 1$.

used to calibrate the tensile strength of the concrete. The result of calibration yields a tensile strength of 4.84 MPa and this leads to a compressive to tensile strength ratio of about 9.14, which is comparable to the experimental observation of 10–11 reported by Hyland and Chen (1970). Note that in this calculation the compressive strength is taken as 44.35 MPa, which is interpreted from Table 3 of Hyland and Chen (1970). Table 2 shows that our solution is capable of predicting the fracture loads for the concrete cylinders of various shapes ($h/b = 0.333$–1) under double-punch of various sizes ($2a = 38$ and 51 mm) with high accuracy. The maximum error in these predictions is only 6.6%.

6. Conclusion

In this paper, we have presented a new elastic solution for a finite isotropic solid circular cylinder of length $2h$ and diameter $2b$ compressed between a pair of concentrically circular punches of diameter $2a$ on the top and bottom end surfaces. This test is called the double-punch test and was first proposed by Chen (1970). Numerical results show that zones of tensile stress concentrations are developed beneath the punches if a/b and Poisson's ratio are small; this observation differs from the common belief that a uniform tensile field is developed between the punches (Chen and Yuan, 1980; Marti, 1989). The maximum tensile stress along the axis decreases with Poisson's ratio and the diameters of the punches

Table 2
Comparison of experimentally observed and the predicted fracture loads in the double-punch tests for concrete[a]

Punch diameter (mm)	Set No. in Hyland and Chen (1970)	Height of specimen (mm)	Double-punch force (kN)	
			Experiment	Theory (error %)
38	14	153.0	161.1	161.1 (0)
	15	76.5	142.4	133.0 (6.6)
	16	51.0	119.1	120.0 (0.7)
51	17	153.0	175.1	185.0 (5.6)
	18	76.5	158.1	164.0 (3.7)

[a] The experimental data are obtained from Table 2 of Hyland and Chen (1970), and $2b = 153$ mm for all specimens. The first data has been used for the calibration of the tensile strength, and $\nu = 0.175$ is assumed in our calculation.

and the cylinder, but is relatively insensitive to the shape of the cylinder. These predictions on the effects of the diameters of the punches and cylinder, and the shape of cylinder agrees with the experimental observations by Chen and Yuan (1980) and Marti (1989). Our numerical results show that the estimation by Bortolotti's (1988) formula is comparable to our prediction for $a/b > 0.25$, but appears to underestimate the tensile strength for smaller a/b. Comparison of our solution with the formula given by Chen (1970) suggests that the formula may underestimate the tensile strength interpreted from the double-punch test. In addition, the fracture loads observed in the double-punch tests on concrete by Hyland and Chen (1970) can be predicted accurately by the present approach if the maximum tensile stress along the axis of symmetry at fracture is interpreted as the tensile strength of the material.

Although the general analysis given in Part I has only been applied to the stress analysis for the double-punch test in this paper, the general framework given in CW is applicable to the stress analysis of cylinders subjected to any arbitrary loading or testing configuration.

Acknowledgements

This research was supported by the Research Grants Council (RGC) of the Hong Kong SAR Government under the Competitive Earmarked Research Grant (CERG) No. PolyU 70/96E.

Appendix A

The proof for Eq. (10) is outlined here. The axial stress on the end surface can be expanded into (Watson, 1944):

$$\sigma_{zz} = \sum G_s J_0\left(\frac{\lambda_s}{b} r\right) \tag{A1}$$

where G_s is given by

$$G_s = -\frac{2}{b^2 J_0^2(\lambda_s)} \int_0^a r p(r) J_0\left(\frac{\lambda_s}{b} r\right) \mathrm{d}r \tag{A2}$$

where $p(r)$ is given in Eq. (7). Substituting Eq. (7) into Eq. (A2) and applying the change of variable $r = a \sin\theta$, we obtain:

$$G_s = -\frac{P}{b^2 \pi J_0^2(\lambda_s)} \int_0^{\pi/2} \sin\theta J_0\left(\frac{\lambda_s}{b} a \sin\theta\right) \mathrm{d}\theta \tag{A3}$$

This integration can be done exactly by using formula (6.683) of Gradshteyn and Ryzhik (1980) to yield:

$$G_s = -\frac{P}{b^2 \pi J_0^2(\lambda_s)} \left(\frac{ab}{2\lambda_s}\right)^{1/2} \Gamma\left(\frac{1}{2}\right) J_{1/2}\left(\frac{\lambda_s}{b} a\right) \tag{A4}$$

Finally, Eq. (10) can be derived if we note that (e.g. Abramowitz and Stegun, 1965):

$$J_{1/2}(x) = \sqrt{\frac{2}{\pi x}} \sin x \quad \text{and} \quad \Gamma\left(\frac{1}{2}\right) = \sqrt{\pi} \tag{A5}$$

References

Abramowitz, M., Stegun, I.A. (Eds.), 1965. Handbook of Mathematical Functions. Dover, New York.

Bazant, Z.P., 1984. Size effect in blunt fracture: concrete, rock and metal. Journal of Engineering Mechanics, ASCE 110 (4), 518–535.

Bortolotti, L., 1988. Double-punch test for tensile and compressive strengths in concrete. ACI Materials Journal 85-M4, 26–32.

Chau, K.T., 1998. Analytic solutions for diametral point load strength tests. Journal of Engineering Mechanics, ASCE 124 (8), 875–883.

Chau, K.T., Wei, X.X., 1999a. Spherically isotropic, elastic spheres subject to diametral point load strength test. International Journal of Solids Structures 36 (29), 4473–4496.

Chau, K.T., Wei, X.X., 1999b. A new analytic solution for the diametral point load strength test on finite solid circular cylinders. International Journal of Solids and Structures, submitted.

Chau, K.T., Wei, X.X., 1999c. Finite solid circular cylinders subjected to arbitrary surface load. Part I: Analytic solution. International Journal of Solids and Structures, in press.

Chen, A.C.T., Chen, W.F., 1976. Nonlinear analysis of concrete splitting tests. Computers and Structures 6, 451–457.

Chen, W.F., 1970. Double punch test for tensile strength of concrete. ACI Materials Journal 67 (2), 993–995.

Chen, W.F., 1975. Limit Analysis and Soil Plasticity. Elsevier, Amsterdam.

Chen, W.F., Colgrove, T.A., 1974. Double-punch test for tensile strength of concrete. Transportation Research Record 504, 43–50.

Chen, W.F., Drucker, D.C., 1969. Bearing capacity of concrete blocks or rock. Journal of the Engineering Mechanics Division, ASCE 95, EM4, 955–978.

Chen, W.F., Trumbauer, B.E., 1972. Double-punch test and tensile strength of concrete. Journals of Materials, American Society of Testing and Materials 7 (2), 148–154.

Chen, W.F., Yuan, R.L., 1980. Tensile strength of concrete: double-punch test. Journal of the Structural Division, ASCE 106, 1673–1693.

Gradshteyn, I.S., Ryzhik, I.M., 1980. Table of Integrals, Series, and Products, Corrected and Enlarged ed. Academic Press, New York, NY.

Hyland, M.W., Chen, W.F., 1970. Bearing capacity of concrete blocks. ACI Journal 67 (3), 228–236.

Marti, P., 1989. Size effect in double-punch tests on concrete cylinders. ACI Materials Journal 86-M58, 597–601.

Neville, A.M., 1978. Properties of Concrete, 2nd ed. ELBS, Pitman, London.

Sneddon, I.N., 1951. Fourier Transforms. McGraw-Hill, New York.

Watson, G.N., 1944. A Treatise on the Theory of Bessel Functions, 2nd ed. Cambridge University Press, Cambridge.

Wei, X.X., Chau, K.T., 1998. Spherically isotropic spheres subject to diametral point load test: analytic solutions. International Journal of Rock Mechanics and Mining Science 35 (4–5), Paper No. 006.

Wei, X.X., Chau, K.T., Wong, R.H.C., 1999. A new analytic solution for the axial point load strength test for solid circular cylinders. Journal of Engineering Mechanics, ASCE 125 (12), 1349–1357.

Wijk, G., 1978. Some new theoretical aspects of indirect measurements of the tensile strength of rocks. International Journal of Rock Mechanics and Mining Science and Geomechanics Abstract 15, 149–160.